

RESEARCH

Open Access



ER membrane receptor FgGET2 plays critical roles in hyphal growth, asexual development, stress responses, and pathogenicity of *Fusarium graminearum*

Caihong Liu^{1,2,3}, Lu Lei², Jing Zhu², Mi Zhang², Ziyi Zhang², Shijing Peng², Jie Tang², Lirun Chen², Qing Chen², Li Kong², Yunfeng Jiang², Guoyue Chen², Qiantao Jiang², Yazhou Zhang², Qiang Xu², Youliang Zheng², Karl-Heinz Kogel^{3,4}, Yuming Wei^{2*} and Pengfei Qi^{2*} 

Abstract

Fusarium graminearum is the major causal agent of Fusarium head blight (FHB), a disease that considerably decreases wheat yield and quality. GET2 is an endoplasmic reticulum (ER) membrane receptor protein in the guided entry of tail-anchored (TA) proteins (GET) pathway, which is the most widely studied post-translational pathway for targeting and inserting TA proteins into the ER. Previous studies indicated that GET2 and its homologs play diverse biological roles in different organisms, including fungi, mammals, and plants. In this study, integrated biochemical, microbiological, and molecular genetic approaches were used to investigate the roles of GET2 in *F. graminearum* (FgGET2). FgGET2 has a conserved primary structure and is localized in the ER. In the *Saccharomyces cerevisiae* Δ ScGET2 mutant, the ectopic expression of FgGET2 restored normal growth. Deleting FgGET2 in *F. graminearum* had detrimental effects on vegetative growth polarity, vacuolar morphology, and conidial production, morphology, and germination. In addition, the lack of FgGET2 expression disrupted responses to different stress conditions (treatments with environmental stressors, e.g., metals, fungicides, the ER stressor, and DNA replication and damage stressors) to varying degrees. Furthermore, deleting FgGET2 in *F. graminearum* resulted in decreased pathogenicity on wheat spikes but increased deoxynivalenol production in wheat spikes and liquid medium. Re-introducing a functional FgGET2 into Δ FgGET2 recovered the wild-type phenotype. Collectively, these findings underscore the critical roles of FgGET2 in influencing diverse cellular and biological processes essential for *F. graminearum* growth and pathogenicity.

Keywords GET pathway, *Fusarium graminearum*, FgGET2, Stress responses, Pathogenicity

*Correspondence:

Yuming Wei

ymwei@sicau.edu.cn

Pengfei Qi

pengfeiqi@hotmail.com

Full list of author information is available at the end of the article



© The Author(s) 2025. **Open Access** This article is licensed under a Creative Commons Attribution 4.0 International License, which permits use, sharing, adaptation, distribution and reproduction in any medium or format, as long as you give appropriate credit to the original author(s) and the source, provide a link to the Creative Commons licence, and indicate if changes were made. The images or other third party material in this article are included in the article's Creative Commons licence, unless indicated otherwise in a credit line to the material. If material is not included in the article's Creative Commons licence and your intended use is not permitted by statutory regulation or exceeds the permitted use, you will need to obtain permission directly from the copyright holder. To view a copy of this licence, visit <http://creativecommons.org/licenses/by/4.0/>.

Background

Fusarium head blight (FHB) of wheat is a devastating disease that is primarily caused by the filamentous fungus *Fusarium graminearum* (Xu and Nicholson 2009; Dean et al. 2012). This disease decreases grain yield but also threatens human and animal health because of the presence of mycotoxins, such as deoxynivalenol (DON), in contaminated grains (Vidal et al. 2018; Chen et al. 2019; Duan et al. 2020). There is currently no wheat germplasm immune to FHB; the wheat germplasm most tolerant to FHB is only able to delay the spread of the pathogenic fungus within spikes (Li et al. 2019; Su et al. 2019). Hence, the application of synthetic chemical fungicides is still the major strategy for controlling FHB. However, because there are only a few effective fungicides with different modes of action, their continued use may lead to *F. graminearum* developing increased tolerance or even resistance, making them less effective for controlling FHB. Therefore, clarifying the molecular mechanisms underlying *F. graminearum* pathogenicity is essential for efficient FHB management.

The guided entry of tail-anchored (TA) proteins (GET) pathway in yeast (*Saccharomyces cerevisiae*) is the most extensively studied post-translational pathway for targeting and inserting TA proteins, a unique class of integral membrane proteins, into the endoplasmic reticulum (ER) (Chio et al. 2017; Mateja et al. 2018). In this pathway, a pre-targeting complex receives the TA protein from the ribosome and transfers it to the homodimeric ATPase ScGET3, resulting in the formation of a targeting complex (TA-ScGET3) in the cytoplasm (Chang et al. 2010; Suloway et al. 2012). ScGET2, an ER membrane receptor protein, may capture this TA-ScGET3 complex in the cytoplasm (Wang et al. 2011; McDowell et al. 2020). Subsequently, ScGET2 combines with another ER membrane receptor protein, ScGET1, to form a receptor complex that facilitates the terminal integration of TA proteins into the ER membrane (Yamamoto and Sakisaka 2012; Zalisko et al. 2017; Heo et al. 2023).

In mammals, the transmembrane domain recognition complex (TRC) targeting pathway is homologous to the GET pathway, with the calcium-modulating cyclophilin ligand protein-encoding gene (*CAML*) functionally equivalent to *ScGET2* (Vilardi et al. 2011; Yamamoto and Sakisaka 2012). However, because of the diversity in their amino acid (aa) sequences, *CAML* and *ScGET2* were not initially considered homologs (Yamamoto and Sakisaka 2012). It was only after an analysis using a position-specific iterated (PSI)-basic local alignment search tool (BLAST) that *CAML* and *ScGET2* were revealed to have a common evolutionary origin. Their homologs are relatively ubiquitous among eukaryotes

(Borgese 2020). Subsequently, *AtGET2* in *Arabidopsis thaliana* was identified on the basis of its function and physical interactions with other GET pathway components, providing a new aa sequence that is better for identifying homologs in different eukaryotic groups, including ascomycetes (Asseck et al. 2021).

GET2 proteins in different eukaryotes exhibit equally low sequence conservation, but they share the same overall topology, including a cytosolic domain (CD) at the N terminus, three transmembrane domains (TMDs), and a luminal C terminus (Carvalho et al. 2019; Asseck et al. 2021). Most importantly, near the N terminus, there is a cluster of positively charged aa (at least four consecutive arginine or lysine residues) that is highly conserved among eukaryotes (Carvalho et al. 2019; Asseck et al. 2021). This motif is indispensable for the binding to ScGET3 (Stefer et al. 2011) and its homologs in both mammals (Yamamoto and Sakisaka 2012) and plants (Asseck et al. 2021). An earlier analysis of GET2 sequences in ascomycetes detected the motif R/KER/K in the N-terminal region (Asseck et al. 2021).

In *S. cerevisiae*, the *ScGET2* knock-out (KO) mutant ($\Delta ScGET2$) exhibited pleiotropic defects, including improper protein retention in the ER, decreased cell growth under various stress conditions (Schuldiner et al. 2008; Kiktev et al. 2012), abnormal mitochondrial morphology and mitophagy (Dimmer et al. 2002; Okreglak and Walter 2014; Onishi et al. 2018), and defective meiotic nuclear division (Enyenihi and Saunders 2003; Auld et al. 2006). In mammals, *CAML* has been identified as a regulator of numerous signal transduction systems (Yamamoto and Sakisaka 2012). Its KO mutants exhibited early embryonic lethality (Tran et al. 2003). Moreover, a lack of *CAML* expression in the inner ear led to a severe loss of cochlear hair cells and complete deafness (Bryda et al. 2012). In *A. thaliana*, *AtGET2* KO mutant seedlings showed shorter root hairs than wild-type (WT) seedlings (Asseck et al. 2021). Furthermore, *PfGET2* in the human malaria parasite *Plasmodium falciparum* can rescue the $CuSO_4$ -sensitive phenotype of the $\Delta ScGET2$ mutant (Kumar et al. 2021). Despite these findings, the biological role of GET2 in filamentous fungi remains unclear.

In this study, we identified the physiological consequences of losing a functional *GET2* in *F. graminearum*. We determined that *FgGET2* is required for various processes, including vegetative growth, vacuole morphogenesis, multiple stress responses, asexual development, and pathogenicity. These findings may be useful for developing effective strategies for minimizing the threat of FHB.

Results

Identification of *GET2* in *F. graminearum*

To identify the *FgGET2* gene, the deduced aa sequences of ScGET2 from *S. cerevisiae* (Protein ID NP_011006.1), AtGET2 from *A. thaliana* (NP_567900.1), CAML from *Homo sapiens* (NP_001736.1), and PfGET2 from *P. falciparum* (XP_001349661.1) were used for BLAST searches for their homologs in *F. graminearum*. These searches identified FGSG_06264 (XP_011324914.1) as the sole candidate. Because of the diversity and low sequence similarity in GET2 family sequences across kingdoms, to ensure that authentic homologous genes were not overlooked, proteins in the *F. graminearum* proteome that met the following two conditions (Fig. 1a) were identified: (i) presence of the R(K)ER(K)R motif, which is a representative conserved motif in ascomycetes (Asseck et al. 2021), within 50 aa of the N terminus and (ii) presence of three TMDs. Employing this strategy, FGSG_06264 was also retrieved as the sole hit (Fig. 1a).

The full-length *FgGET2* sequence consists of 1067 bp, which includes a 59 bp intron. It encodes a polypeptide comprising 335 aa, with a highly conserved protein domain structure similar to that of other GET2 proteins (Fig. 1b). Although the aa sequence similarity between

FgGET2 and ScGET2, AtGET2, PfGET2, and CAML was relatively low (i.e., sequence identities of 16, 15, 8, and 12%, respectively), a conserved group of positively charged aa residues near the N terminus was detected in all of these proteins (Fig. 1b).

Subcellular localization of *FgGET2* in *F. graminearum*

We determined the subcellular localization of *FgGET2* using the *F. graminearum* strain overexpressing the *FgGET2*-eGFP fusion protein. The green fluorescence of *FgGET2*-eGFP was detected in conidia (Fig. 2a), conidia germinated in liquid yeast extract peptone dextrose (YEPD) medium for 6 h (Fig. 2b), and hyphae grown in liquid YEPD medium for 24 h (Fig. 2c). Notably, in hyphae, *FgGET2*-eGFP was co-localized with the ER-Tracker Red signal (Fig. 2c), indicating that *FgGET2* is localized to the ER, similar to other GET2 proteins.

FgGET2 restores the defective growth of the yeast Δ ScGET2 mutant

An earlier study revealed phenotypic changes in the Δ ScGET2 mutant under various stress conditions (Schuldiner et al. 2008). To determine whether *FgGET2* can compensate for the deletion of *GET2* in Δ ScGET2,

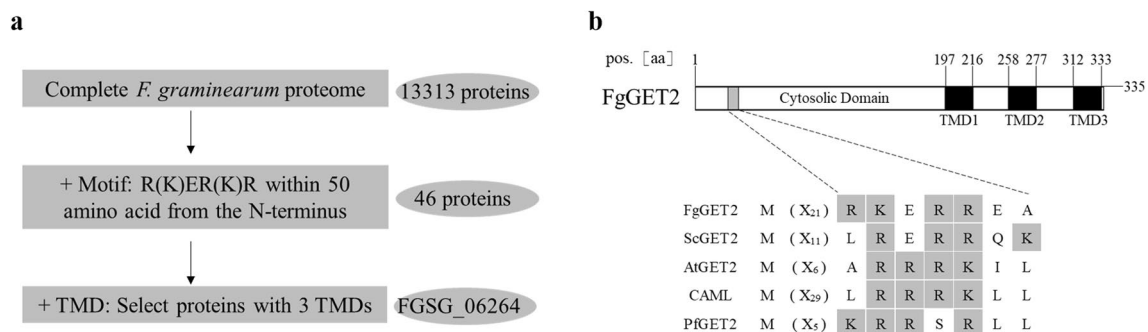


Fig. 1 Identification of *GET2* in *F. graminearum*. **a** Flowchart illustrating the bioinformatics-based prediction of *FgGET2* in the *F. graminearum* proteome. **b** *FgGET2* domain structure and positively charged motifs characterized by four consecutive arginine or lysine residues in the N terminus of ScGET2, AtGET2, CAML, and PfGET2. Arginine (R) and lysine (K) are highlighted in gray. aa, amino acid; TMD, transmembrane domain

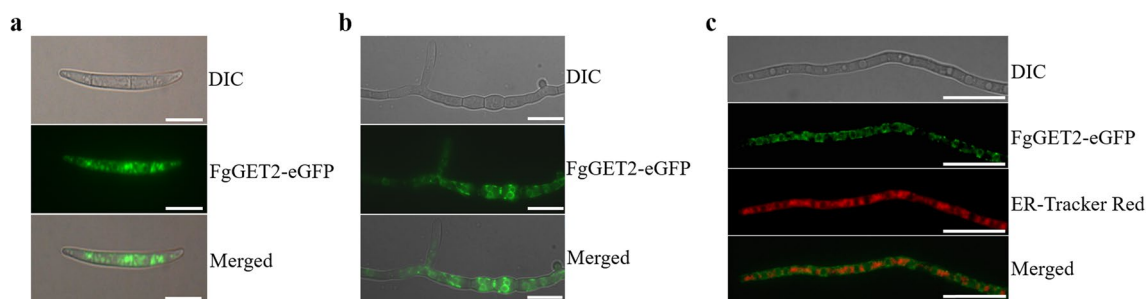


Fig. 2 Subcellular localization of *FgGET2*. **a** Green fluorescence in conidia. **b** Green fluorescence in germinating conidia. **c** Co-localization of *FgGET2* and ER-Tracker Red in vegetative hyphae. Bar, 10 μ m; DIC, differential interference contrast

the expression vector pYES2-*FgGET2* containing the full-length *FgGET2* cDNA sequence was constructed and inserted into Δ *ScGET2*. As controls, Δ *ScGET2* was transformed with pYES2-*ScGET2* (positive control) and the empty pYES2 vector (negative control). As expected, WT yeast cells grew well on YEPD medium regardless of the presence of different stressors, whereas Δ *ScGET2* cell growth was significantly compromised in the presence of hydroxyurea, tunicamycin, hygromycin, or CuSO₄ and at 39°C (i.e., heat stress). Notably, the defective growth of Δ *ScGET2* was resolved by the transformation of mutant

cells with either pYES2-*ScGET2* or pYES2-*FgGET2*, but not with the empty pYES2 vector (Fig. 3). Accordingly, *ScGET2* and *FgGET2* may have similar functions.

Construction of Δ *FgGET2* and *C-FgGET2* mutants

To elucidate the biological roles of *FgGET2*, we generated the Δ *FgGET2* KO mutant using a homologous recombination strategy (Fig. 4a). Briefly, the *FgGET2*-pRF-HU2 recombinant plasmid (hygromycin resistance) was constructed (Fig. 4b) and transformed into the WT strain. The *FgGET2* coding sequence was replaced with the

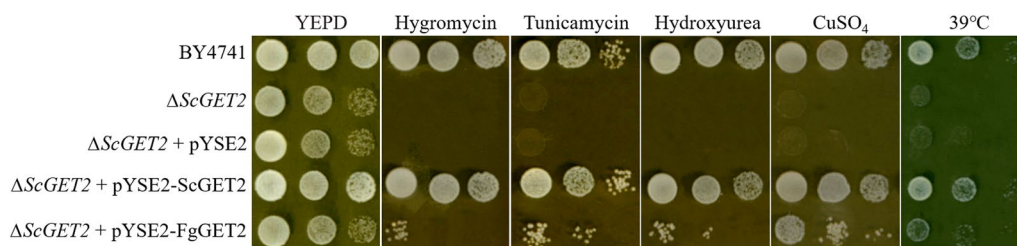


Fig. 3 *FgGET2* rescues the growth defects of the Δ *ScGET2* mutant. Δ *ScGET2* was transformed with pYES2-*ScGET2* and pYES2-*FgGET2*. WT strain BY4741 and Δ *ScGET2* transformed with empty pYES2 were used as controls. For each strain, cell suspensions (different dilutions) were spotted on YEPD medium supplemented with the indicated stress agents: 200 mM hygromycin, 2 μg/mL tunicamycin, and 200 μg/mL hydroxyurea at 30°C; 3 mM CuSO₄ at 37°C. For the heat sensitivity assay, yeast strains were grown at 39°C. The growth of each strain was assessed after a 3-day incubation

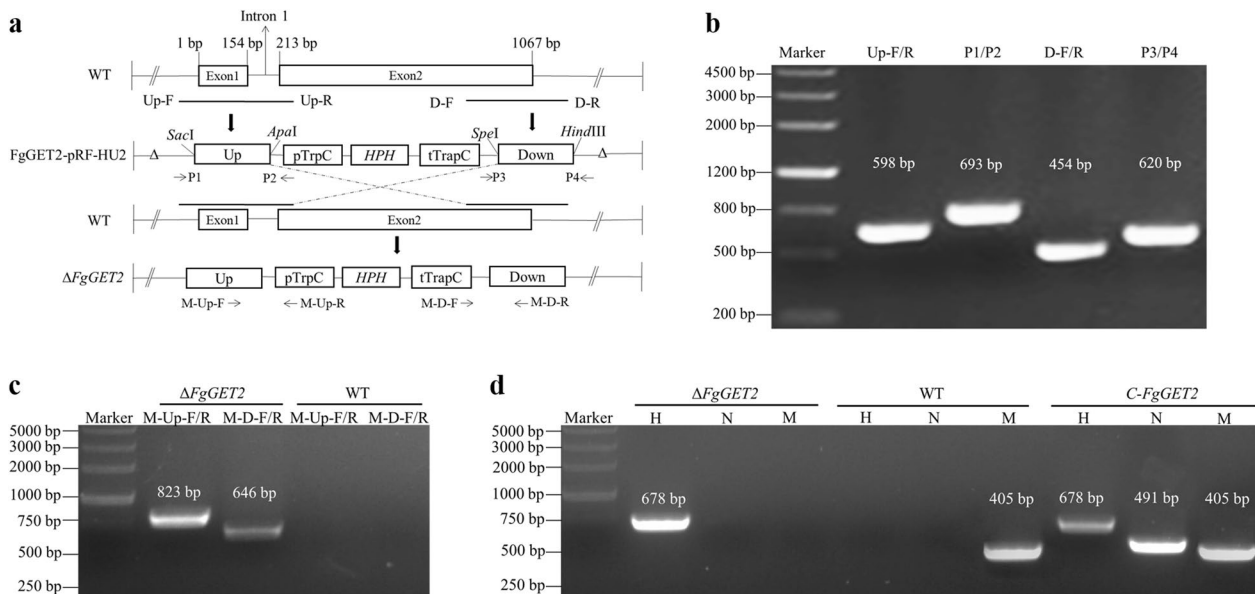


Fig. 4 Production of Δ *FgGET2* and *C-FgGET2* mutants. **a** Constructs and gene structures for disrupting *FgGET2*. The upstream (Up) and downstream (Down) flanking sequences were amplified by PCR using DNA from the wild-type (WT) strain and Up-F/R and D-F/R primer pairs, respectively, and then cloned into the pRF-HU2 vector to construct the *FgGET2*-pRF-HU2 plasmid. *SacI*, *ApaI*, *SpeI*, and *HindIII* indicate the restriction enzymes used. Δ *FgGET2* mutants were generated by replacing *FgGET2* in WT with the hygromycin phosphotransferase (*HPH*)-encoding gene. **b** Validation of *FgGET2*-pRF-HU2 using primer pairs Up-F/R, D-F/R, P1/P2, and P3/P4. **c** PCR verification of Δ *FgGET2* using primer pairs M-Up-F/R and M-D-F/R. **d** Reverse transcription PCR-based verification of the expression of a hygromycin resistance gene, neomycin resistance gene, and *FgGET2* in Δ *FgGET2*, WT, and *C-FgGET2* using primers *HPH*-F/R(H), *NEO*-F/R (N), and M-*FgGET2*-F/R (M), respectively

hygromycin phosphotransferase (HPH)-encoding gene via homologous recombination (Fig. 4a). Hygromycin-resistant transformants were confirmed by a polymerase chain reaction (PCR) amplification (Fig. 4c).

To obtain the complemented mutant, the JM45-*FgGET2* plasmid (neomycin resistance) carrying a 2.4-kb region containing the *FgGET2* coding sequence and its promoter sequence was constructed and inserted into the $\Delta FgGET2$ mutant. The complemented mutant (designated *C-FgGET2*), which was resistant to both hygromycin and neomycin, was identified on the basis of reverse transcription (RT)-PCR (Fig. 4d). According to the RT-PCR results, *FgGET2* was not expressed in $\Delta FgGET2$, but was expressed normally in *C-FgGET2* as in the WT control (Fig. 4d). Hence, *FgGET2* was correctly removed from the genome of $\Delta FgGET2$ and was successfully re-introduced in *C-FgGET2*.

***FgGET2* plays crucial roles in vegetative polar growth and vacuole fusion**

During the *F. graminearum* life cycle, hyphal growth is critical for survival (Riquelme et al. 2018). To assess the importance of *FgGET2* for vegetative growth, WT, $\Delta FgGET2$, and *C-FgGET2* strains were cultured on potato dextrose agar (PDA) and modified synthetischer nährstoffarmer agar (mSNA) media. After 4 days, the growth rate of $\Delta FgGET2$ was significantly lower than that of the

other two strains on both media (Fig. 5a, b). Microscopic examinations revealed $\Delta FgGET2$ produced crooked and narrow hyphae with multiple branches at the hyphal tips (Fig. 5c), suggesting that *FgGET2* is important for maintaining hyphal tip polarity.

An examination using a transmission electron microscope detected small, fragmented vacuoles with numerous irregular spheroids in more than 90% of $\Delta FgGET2$ hyphal cells, whereas approximately 70% of WT hyphal cells contained a single large vacuole (Fig. 5d). The presence of fragmented vacuoles was confirmed by staining hyphae with the vacuole marker 7-amino-4-chloromethylcoumarin (CMAC) (Fig. 5e). These results suggest *FgGET2* may also be important for vacuole fusion in *F. graminearum*.

***FgGET2* affects conidia production, morphology, and germination**

Conidia are critical for the spread of disease in the field (Osborne and Stein 2007). To compare the conidia production of WT, $\Delta FgGET2$, and *C-FgGET2* strains, liquid carboxymethylcellulose (CMC) medium was inoculated with equal amounts of fresh mycelia from each strain. After 4 days, $\Delta FgGET2$ mycelia were relatively thick and aggregated in the culture, whereas WT and *C-FgGET2* mycelia were uniformly dispersed (Fig. 6a). WT and *C-FgGET2* conidia formed on phialides. In contrast,

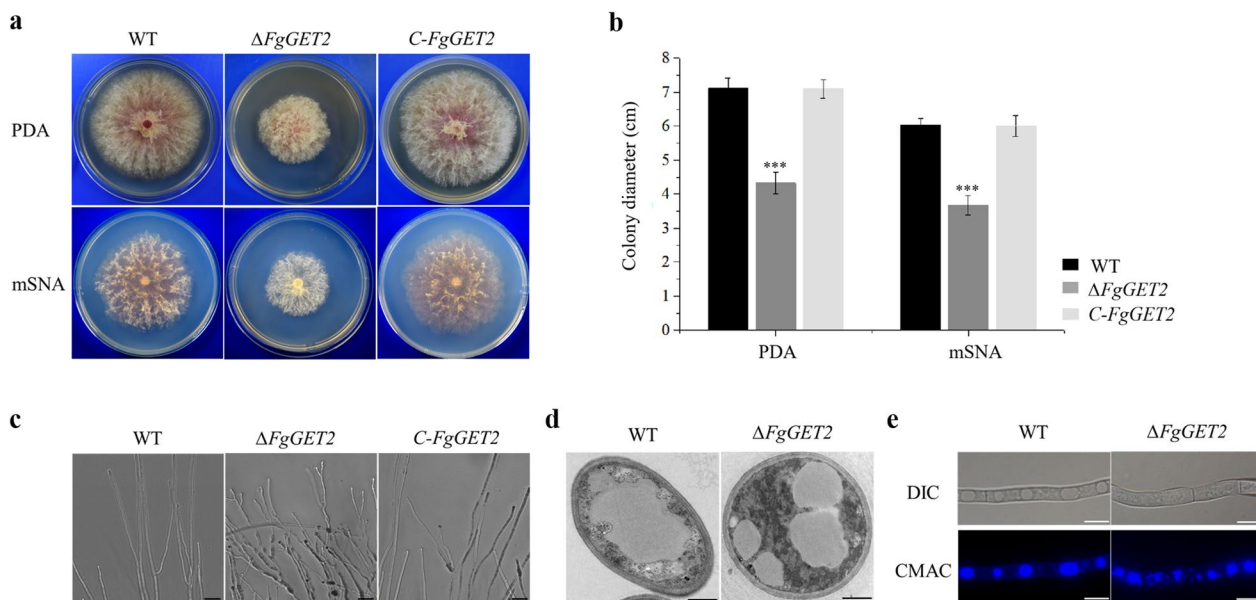


Fig. 5 *FgGET2* is required for vegetative growth and vacuole morphology. **a** WT, $\Delta FgGET2$, and *C-FgGET2* mycelial growth on PDA and mSNA media incubated for 4 days at 25°C in darkness. **b** Colony diameters on PDA and mSNA media. Data were analyzed by Student's *t*-test (***) $P < 0.001$. Means and standard deviations were calculated for three replicates. **c** WT, $\Delta FgGET2$, and *C-FgGET2* hyphal tip and branching patterns on PDA medium. Bar, 20 μ m. **d** Vacuole structures in WT and $\Delta FgGET2$ hyphae as observed using a transmission electron microscope. Bar, 1 μ m. **e** WT and $\Delta FgGET2$ hyphae stained with a vacuole-tracking dye (CMAC) and examined using a fluorescence microscope. DIC, differential interference contrast. Bar, 10 μ m

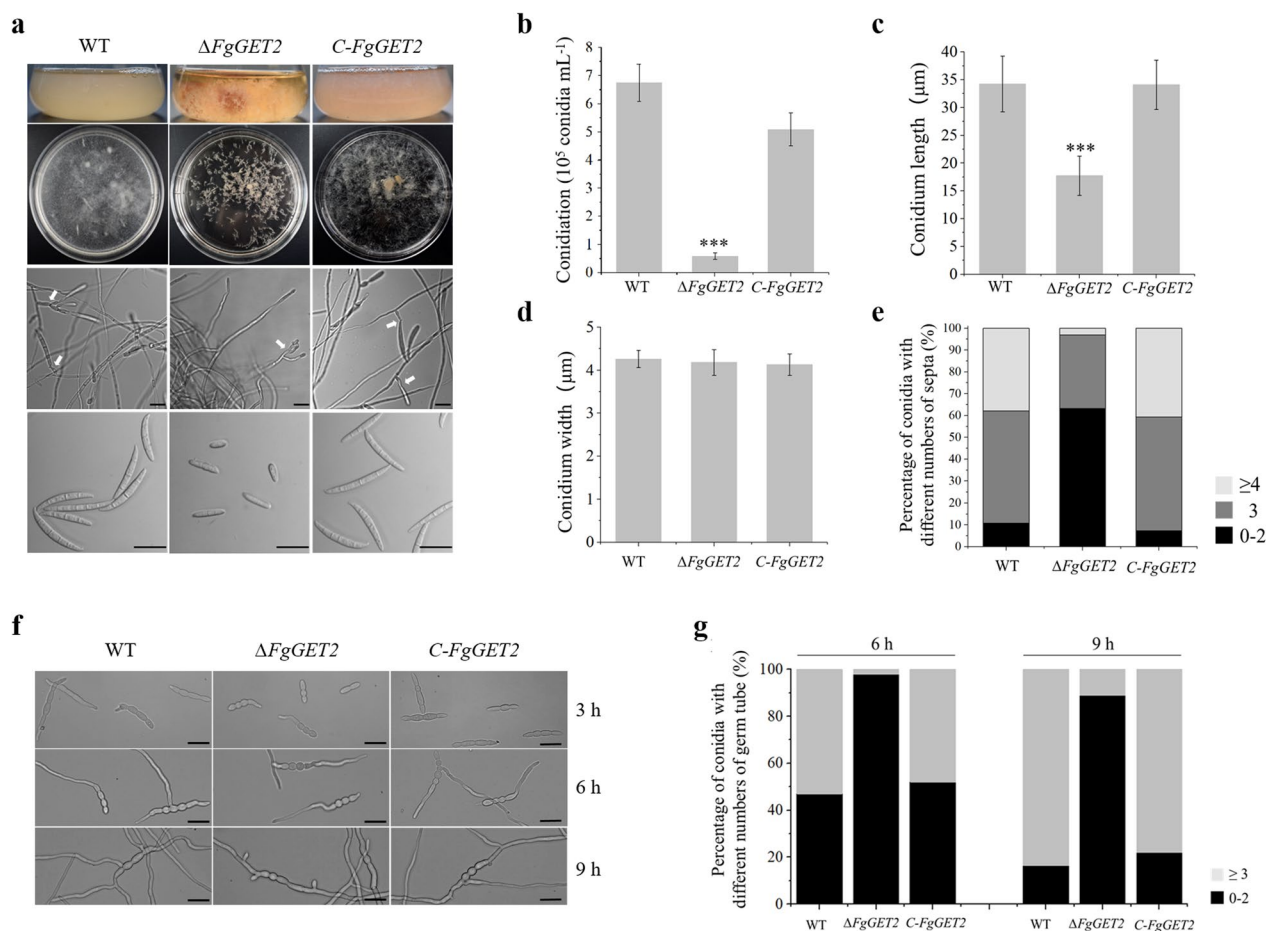


Fig. 6 Comparison of WT, $\Delta FgGET2$, and *C-FgGET2* conidial production and germination. **a** Mycelia, phialides (indicated by white arrows), and conidial morphology in CMC liquid medium. Bar, 20 μ m. **b** Quantification of conidia produced by WT, $\Delta FgGET2$, and *C-FgGET2* strains. Comparisons of conidial length (**c**) and width (**d**), with at least 300 conidia examined per strain. Data were analyzed using Student's *t*-test (***) $P < 0.001$. Means and standard deviations were calculated for three replicates. **e** Percentage of conidia with different numbers of septa. A total of 300 conidia were examined per strain. **f** Morphology of germinated conidia at 3, 6, and 9 h in YEPD medium. Bar, 20 μ m. **g** Percentage of conidia with different numbers of germ tubes at 6 and 9 h after germination. A total of 300 germinated conidia were examined per strain at each time point

phialides were rarely observed in $\Delta FgGET2$ (Fig. 6a). In addition, foot cells were present in WT and *C-FgGET2* conidia but not in $\Delta FgGET2$ conidia (Fig. 6a). The number of conidia produced by $\Delta FgGET2$ decreased by more than 90% compared to that of WT and *C-FgGET2* (Fig. 6b). A microscopic examination of 300 conidia per strain showed that $\Delta FgGET2$ conidia were shorter (Fig. 6c) and had fewer septa (Fig. 6e) than WT and *C-FgGET2* conidia, but there was no significant difference in conidial width (Fig. 6d). Considered together, these results showed that *FgGET2* affects conidial production and morphology in *F. graminearum*.

To determine whether *FgGET2* contributes to conidial germination, liquid YEPD medium was inoculated with conidia (Fig. 6f). Although $\Delta FgGET2$ conidia germinated, the germination was significantly delayed. At 6 h, only 9% of $\Delta FgGET2$ conidia produced three or more germ tubes,

whereas more than 40% of WT and *C-FgGET2* conidia had at least three germ tubes. At 9 h, 25% of $\Delta FgGET2$ conidia produced three or more germ tubes, which was considerably lower than the corresponding percentage of WT and *C-FgGET2* conidia (>80%) (Fig. 6g). These results demonstrate that *FgGET2* influences conidial germination and germ tube polarity in *F. graminearum*.

FgGET2 is essential for *F. graminearum* stress responses

Sensitivity to environmental stresses is a critical factor modulating *F. graminearum* hyphal development and pathogenicity (Chong et al. 2020). Moreover, impaired vacuole fusion affects stress responses in fungi (Yu et al. 2014; Liu et al. 2017). Therefore, $\Delta FgGET2$ responses to several environmental stresses were examined (Fig. 7a, e). After 4 days on PDA medium supplemented with osmotic (1 M NaCl and 1 M D-Sorbitol) and oxidative

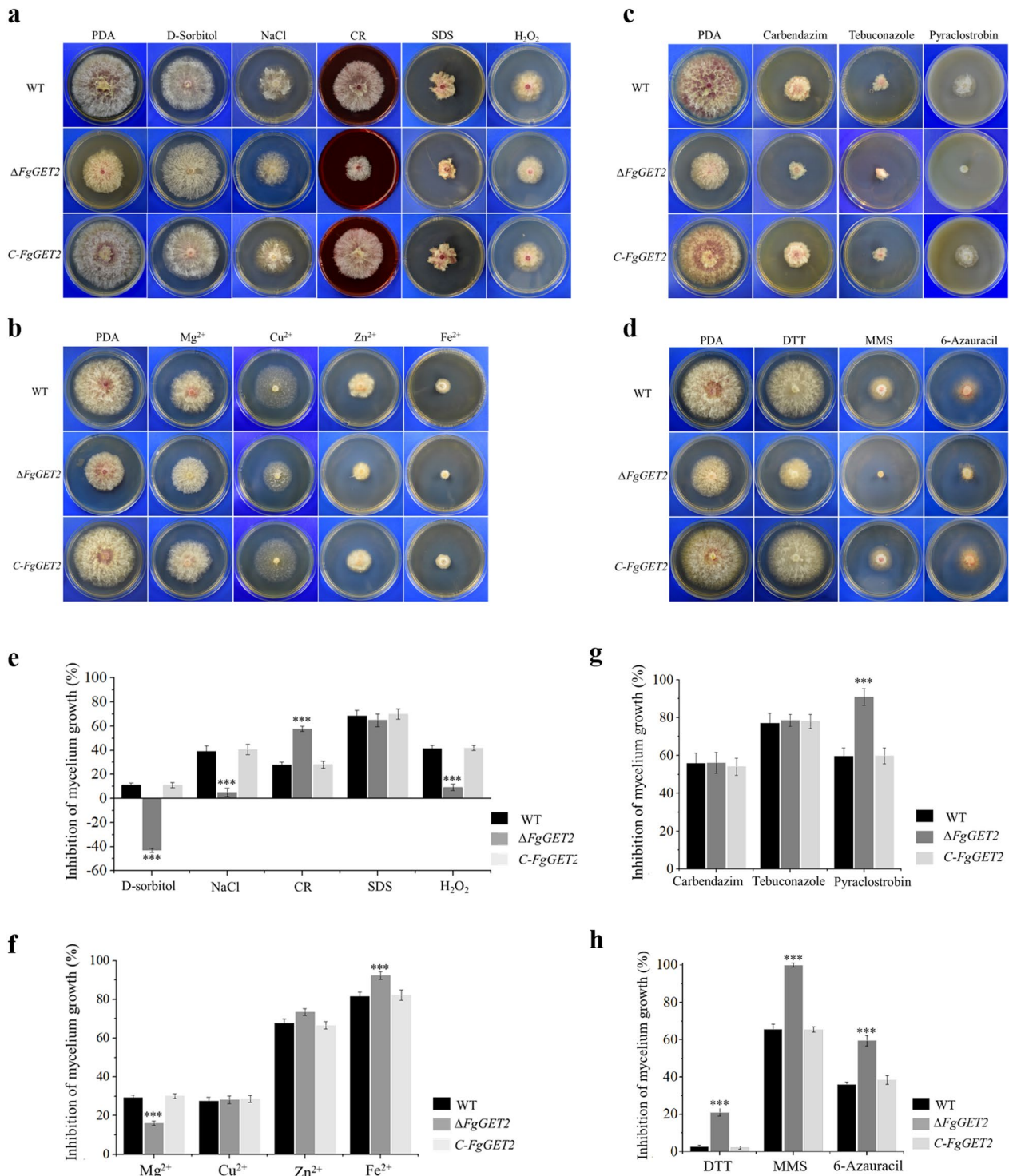


Fig. 7 WT, $\Delta FgGET2$, and *C-FgGET2* vegetative growth under different stress conditions. Strains were grown on PDA medium supplemented with **a** 1 M NaCl and 1 M D-Sorbitol, 0.05% H₂O₂, 0.5 mM Congo Red (CR), and 0.025% sodium dodecyl sulfate (SDS), **b** 0.4 M Mg²⁺, 5 mM Cu²⁺, 10 mM Zn²⁺, and 10 mM Fe²⁺, **c** 0.4 μg/mL carbendazim, 5 μg/mL tebuconazole, and 0.6 μg/mL pyraclostrobin, **d** 5 mM DTT, 100 μg/mL methyl methanesulfonate (MMS), and 100 μg/mL 6-Azauracil. All strains were grown at 25°C for 4 days. **e, f, g,** and **h** Inhibition of mycelial growth for each strain exposed to individual stresses. Data were analyzed using Student's *t*-test (** *P* < 0.01; *** *P* < 0.001). Means and standard deviations were calculated for three replicates

(0.05% H₂O₂) stressors, the growth inhibition rate of $\Delta FgGET2$ was significantly lower than that of WT or *C-FgGET2*. Under cell wall stress conditions, $\Delta FgGET2$ showed increased sensitivity to 0.5 mM Congo Red (CR), but not to 0.025% sodium dodecyl sulfate. Under metal stress conditions, the sensitivity of $\Delta FgGET2$ mycelia to 5 mM Cu²⁺ and 10 mM Zn²⁺ was unaffected. However, $\Delta FgGET2$ exhibited increased tolerance to 0.4 M Mg²⁺ and increased sensitivity to 10 mM Fe²⁺ (Fig. 7b, f). Furthermore, in a fungicide sensitivity assay, $\Delta FgGET2$ exhibited increased sensitivity to 0.6 μ g/mL pyraclostrobin, but not to 0.4 μ g/mL carbendazim or 5 μ g/mL tebuconazole (Fig. 7c, g). These results suggest that *FgGET2* is involved in regulating *F. graminearum* responses to osmotic and oxidative stresses to maintain cell wall integrity and cellular metal homeostasis, while also enhancing fungicide resistance.

Deleting *ScGET2* can lead to defects in DNA replication or DNA damage in *S. cerevisiae* (Zewail et al. 2003). Therefore, we examined the response of $\Delta FgGET2$ to 100 μ g/mL methyl methanesulfonate (MMS) and 100 μ g/mL 6-Azauracil, which are known to damage DNA. As expected, $\Delta FgGET2$ exhibited increased sensitivity to these DNA-damaging agents (Fig. 7d, h). In yeast, a loss-of-function deletion to *ScGET2* reportedly results in the cytoplasmic aggregation of unfolded ER-destined TA proteins, leading to ER stress (Schuldiner et al. 2008). To investigate whether the deletion of *FgGET2* in *F. graminearum* also triggers ER stress, we analyzed $\Delta FgGET2$ grown on PDA medium containing the ER stressor dithiothreitol (DTT). We observed that $\Delta FgGET2$ exhibited increased sensitivity to 5 mM DTT.

***FgGET2* affects fungal pathogenicity and DON biosynthesis**

To determine the effect of *FgGET2* on pathogenicity, flowering wheat heads were inoculated with 1×10^3 conidia. At 12 days post-inoculation (dpi), obvious head blight symptoms were detected throughout the spikes inoculated with WT or *C-FgGET2*, whereas disease symptoms in the spikes inoculated with $\Delta FgGET2$ were restricted to the spikelets (Fig. 8a, b). At 2 dpi, the fungal biomass of the spikes inoculated with $\Delta FgGET2$ was significantly lower than that of the spikes inoculated with WT and *C-FgGET2* (Fig. 8c). To further analyze the effect of *FgGET2* on the penetration behavior of *F. graminearum*, $\Delta FgGET2$, WT, and *C-FgGET2* were grown on cellophane membranes placed on PDA medium. The ability of $\Delta FgGET2$ to penetrate cellophane was weaker than that of WT or *C-FgGET2* (Fig. 8d, e).

To explore how *FgGET2* influences mycotoxin production, the amount of DON in infected wheat spikes was quantified at 8 dpi. Compared with the spikes inoculated with WT and *C-FgGET2*, the spikes inoculated

with $\Delta FgGET2$ had significantly less DON (16 and 23% less, respectively) (Fig. 8f) and lower fungal biomass (44 and 47% lower, respectively) (Fig. 8g). Thus, the DON content:fungal biomass ratio was higher for the samples inoculated with $\Delta FgGET2$ than for the samples inoculated with WT or *C-FgGET2*. Hence, the deletion of *FgGET2* enhanced the accumulation of DON in *F. graminearum* on wheat spikes. To confirm this finding, the accumulation of DON was subsequently assayed in liquid medium. As expected, compared with WT, $\Delta FgGET2$ produced approximately threefold more DON (Fig. 8h). In accordance with this finding, the expression levels of DON biosynthesis-related genes (*TRI5*, *TRI6*, and *TRI101*) were up-regulated in $\Delta FgGET2$ (Fig. 8i). A previous study showed that DON production is involved in the formation of intercalary swollen hyphal compartments (Jiang et al. 2016). Therefore, $\Delta FgGET2$, WT, and *C-FgGET2* hyphae were compared in terms of morphology under DON-inducing conditions. Unexpectedly, there were no obvious differences in hyphal structures and bulbous numbers (Fig. 8j). These results indicate that the increased DON production in liquid medium was achieved by triggering the expression of *TRI* genes rather than by altering the structure of DON-producing hyphae. On the basis of these findings, we conclude that *FgGET2* is essential for the penetration of wheat plants and subsequent spread as well as the production of DON in wheat spikes and liquid medium.

Discussion

The ER membrane receptor *ScGET2* in the GET pathway in yeast and *CAML* in the TRC pathway of vertebrates mediate the final step of the process that integrates TA proteins into the ER membrane (Wang et al. 2011). Compared with *GET2* in yeast and mammals, *GET2* in the phytopathogenic fungus *F. graminearum* has not been thoroughly investigated in terms of its biological functions. In this study, we identified and functionally characterized *FgGET2* in *F. graminearum*.

Although the *FgGET2* aa sequence differs considerably from *GET2* sequences in other organisms, it contains a highly conserved protein structure (CD—three TMDs—luminal C terminus), with a cluster of positively charged aa residues near the N terminus (Fig. 1b). In *S. cerevisiae*, the loss of a functional *ScGET2* resulted in a lack of stress tolerance; however, earlier research indicated the simultaneous expression of yeast *ScGET1* with either *AtGET2* or *CAML* can weakly restore the viability of a mutant in which both *ScGET1* and *ScGET2* are knocked out (Vilardi et al. 2011; Asseck et al. 2021). In addition, *PfGET2* of *P. falciparum* can rescue the CuSO₄-sensitivity of the $\Delta ScGET2$ strain (Kumar et al. 2021). In the current study, we determined that, as expected, *FgGET2* can restore the

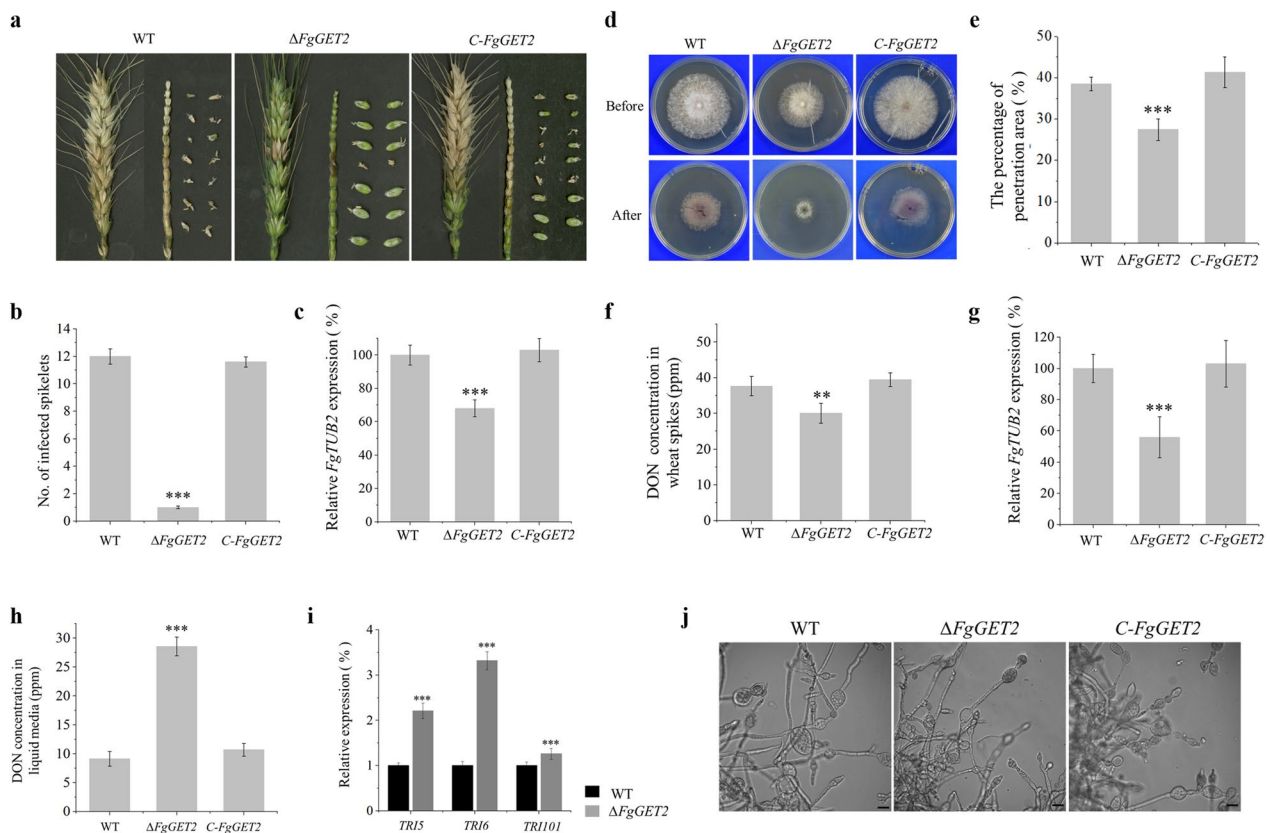


Fig. 8 Effect of *FgGET2* on *F. graminearum* pathogenicity and DON production. **a** Flowering wheat spikes were inoculated with WT, $\Delta FgGET2$, and C-FgGET2 conidial suspensions. Spikes, seeds, and rachises were photographed at 12 dpi. **b** Numbers of infected and bleached spikelets at 12 dpi. **c** Fungal biomass was determined on the basis of the relative expression of *FgTUB2* in spikelets at 2 dpi. **d** Penetration of a cellophane membrane by WT, $\Delta FgGET2$, and C-FgGET2. The indicated strains were grown on top of cellophane membranes on PDA medium for 4 days as a control ('Before' treatment). To assess mycelial growth on the medium, which indicates the cellophane membrane was penetrated, the cellophane with the fungal colony was removed on day 3 and the medium was incubated for an additional day ('After' treatment). **e** Percentages of penetration area for WT, $\Delta FgGET2$, and C-FgGET2 on cellophane membranes. **f** DON production in wheat spikes infected with conidial suspensions of the indicated strains at 8 dpi. **g** Relative expression of *FgTUB2* in the indicated strains in wheat heads at 8 dpi. **h** DON concentration in the supernatants obtained after a 24-h incubation of the indicated strains in liquid medium. **i** Expression of *TRI* genes in WT and $\Delta FgGET2$ hyphae cultured in liquid medium for 24 h. **j** Hyphae bulbous structures of the indicated strains after a 24-h incubation in liquid medium. Bar, 20 μ m. Data were analyzed using Student's *t*-test (** $P < 0.01$; *** $P < 0.001$). Means and standard deviations were calculated for three replicates

mutant phenotype of $\Delta ScGET2$ (Fig. 3). Moreover, similar to other reported GET2 proteins, *FgGET2* is located in the ER (Fig. 2b), providing further evidence that *FgGET2* is indeed a GET2 homolog in *F. graminearum*.

In *S. cerevisiae*, *ScGET2* regulates vegetative growth (Smith et al. 1996; Winzeler et al. 1999), while also mediating responses to diverse abiotic stressors, including cell wall-damaging agents (Hughes et al. 2000), oxidative stress-inducing compounds (Helsen et al. 2020), heavy metals (Ruotolo et al. 2008; Schuldiner et al. 2008), and DNA-damaging compounds (Zewail et al. 2003). *ScGET2* can recruit the TA-*ScGET3* complex from the cytosol to the ER (McDowell et al. 2020). The absence of *ScGET2* leads to the improper insertion of multiple

TA proteins that mediate a wide range of vital cellular activities (Borgese and Fasana 2011), suggesting that the pleiotropic effects of knocking out *ScGET2* might be a secondary consequence of abnormally localized TA proteins (Schuldiner et al. 2008). Promptly unfolded TA proteins aggregate outside the ER and disrupt the response to unfolded proteins. In earlier studies, the $\Delta ScGET2$ mutant exhibited heightened sensitivity to ER stress inducers, including DTT and tunicamycin (Schuldiner et al. 2008; Jonikas et al. 2009). In the present study, defective functions in *F. graminearum* caused by the lack of *FgGET2* expression adversely altered vegetative growth (Fig. 5), asexual development (Fig. 6), and responses to multiple abiotic stresses (Fig. 7). Similarly, the sensitivity

of *F. graminearum* to DTT increased after *FgGET2* was knocked out (Fig. 7d). These findings also suggest that the pleiotropic effects of knocking out *FgGET2* may be associated with TA protein mislocalization, but this will need to be experimentally verified.

F. graminearum pathogenicity depends on a complex network regulated by multiple factors. In $\Delta FgGET2$, impaired hyphal growth, delayed conidial germination, and altered stress sensitivity may influence pathogenicity. On flowering wheat spikes, *FgGET2* expression was essential for hyphal growth in the early infection stages (Fig. 8c) and for the spread through the rachis (Fig. 8a). An analysis of the penetration of a cellophane membrane revealed the importance of *FgGET2* (Fig. 8d, e). In addition, DON is another key pathogenicity factor in *F. graminearum* (Jiang et al. 2016; Chen et al. 2019). Although the total amount of DON in $\Delta FgGET2$ decreased on spikes (Fig. 8f), intriguingly, DON production by $\Delta FgGET2$ mycelia tended to increase on wheat spikes (Fig. 8f, g) and in liquid medium (Fig. 8h), which may be a compensatory mechanism to counterbalance the decreased growth rate and other defects, thereby enabling *F. graminearum* to spread efficiently. Currently, the application of chemical fungicides is still one of the main approaches for controlling FHB. Notably, $\Delta FgGET2$ exhibited increased sensitivity to pyraclostrobin (Fig. 7c, g), suggesting that *FgGET2* may be a potential molecular target for increasing the efficacy of this fungicide.

Conclusions

In summary, our results demonstrate that *FgGET2* encodes a key component of the GET pathway and regulates vegetative growth, asexual development, abiotic stress responses, and pathogenicity in *F. graminearum*.

Methods

Fungal strains and growth conditions

F. graminearum isolate DAOM180378 (Canadian Fungal Culture Collection, AAFC, 270 Ottawa, ON, Canada) is highly virulent in wheat. The colony morphology and growth rate of WT and mutant strains were determined on PDA (Aobox, Beijing, China) and mSNA (1 g KH_2PO_4 , 1 g KNO_3 , 0.5 g $MgSO_4$, 0.5 g KCl, 1 g glucose, 1 g sucrose, and 20 g agar per liter) media at 25°C for 4 days in darkness. Mycelial radial growth was estimated as described by Qi et al. (2012).

To determine the sensitivity of *F. graminearum* to stressors, 5-mm mycelial plugs taken from the edge of a 4-day-old colony were placed on PDA medium supplemented with different stressors (concentrations indicated in figure legends) in Petri dishes. Mycelial radial growth inhibition (RGI) was calculated using the following formula: $RGI (\%) = [(C - N) / (C - 5)] \times 100$ (Jiang et al. 2011),

where C and N represent the colony diameter of the control and treatment, respectively. The experiment was repeated three times, with six Petri dishes per treatment. For the conidiation assay, 20 mg fresh mycelium was used to inoculate 30 mL CMC medium (1 g NH_4NO_3 , 1 g KH_2PO_4 , 0.5 g $MgSO_4 \cdot 7H_2O$, 1 g yeast extract, and 15 g CMC per liter) in a 50 mL flask (Cappellini and Peterson 1965). The inoculated medium was incubated on a shaker (180 rpm) for 5 days, after which the number of conidia in the flask was determined using a hemocytometer. Conidial germination was assessed using freshly harvested conidia cultured in liquid YEPD medium (20 g peptone, 10 g yeast extract, and 20 g dextrose per liter).

Nucleic acid extraction and PCR

Genomic DNA and total RNA were extracted using Plant genomic DNA Mini Kit and Plant genomic RNA Mini Kit (Biofit, Chengdu, China), respectively. The extracted RNA (1 μ g) was reverse transcribed to cDNA using a HiScript III 1st Strand cDNA Synthesis Kit (Vazyme, Nanjing, China). Phanta Max Super-Fidelity DNA Polymerase (Vazyme) was used for PCR and RT-PCR.

To measure the relative fungal biomass in wheat spikelets, the expression of the β -tubulin gene *FgTUB2* (FGSG_09530; primer pair TUB2-F/R) was estimated on the basis of quantitative RT-PCR (qRT-PCR), with a wheat glyceraldehyde-3-phosphate dehydrogenase gene *GAPDH* (Ta.66461; primer pair w-GAPDH-F/R) selected as the reference control for normalizing expression levels. To analyze *TRI* gene expression, RNA was extracted from hyphae in the DON induction liquid medium for a qRT-PCR analysis using gene-specific primer pairs to amplify the trichothecene synthase genes *TRI5* and *TRI6* (*TRI5*-F/R and *TRI6*-F/R, respectively) and the trichothecene acetyltransferase gene *TRI101* (*TRI101*-F/R). *FgTUB2* served as the reference gene. The qRT-PCR analysis was performed using the MyiQ Real-Time PCR Detection System (Bio-Rad, Hercules, CA, USA) and the Taq Pro Universal SYBR qPCR Master Mix (Vazyme) according to the manufacturer's instructions. Transcript levels were calculated using the $2^{-\Delta\Delta C_t}$ method (Livak et al. 2001), with three biological replicates per treatment. The primers used in this study are listed in Additional file 1: Table S1.

Fungal transformation

$\Delta FgGET2$ mutants were produced via *Agrobacterium tumefaciens*-mediated transformation (Maier et al. 2005). To generate the gene replacement construct, the 598 bp upstream and 454 bp downstream flanking sequences were amplified by PCR using *F. graminearum* genomic DNA and Up-F/R and D-F/R primer pairs, respectively. The amplified fragments were cloned

into the pRF-HU2 vector using a ClonExpress II One Step Cloning Kit (Vazyme). The resulting recombinant plasmid FgGET2-pRF-HU2 was analyzed using primer pairs P1/P2 and P3/P4 to verify the accuracy of the inserted sequence. The *FgGET2* gene was replaced by the *HPH* gene using a homologous recombination strategy (Fig. 4a). Hygromycin B (Calbiochem, La Jolla, CA, USA) was added to a final concentration of 100 mg/mL to screen for transformants. Primer pairs M-Up-F/R and M-D-F/R were used to examine the construct in $\Delta FgGET2$ by PCR. Only transformants that underwent homologous recombination in the target region produced the expected PCR products. At least three $\Delta FgGET2$ mutants were used in each of the subsequent experiments.

To restore the *FgGET2* function in $\Delta FgGET2$, a 2.4-kb region containing the coding sequence and its promoter was amplified by PCR using the primer pair C-FgGET2-F/R and then cloned into plasmid JM45. The resulting construct (JM45-FgGET2) was inserted into $\Delta FgGET2$ protoplasts via polyethylene glycol-mediated transformation (Hou et al. 2004). G418 Sulfate (Calbiochem) was added for a final concentration of 300 mg/mL to screen for transformants. The generated C-FgGET2 transformants were identified by RT-PCR, with the primer pairs HPH-F/R, NEO-F/R, and M-FgGET2-F/R used to analyze hygromycin resistance gene, neomycin resistance gene, and *FgGET2* expression, respectively.

To determine the subcellular localization of FgGET2, its coding sequence was amplified by PCR using the primer pair FgGET2-eGFP-F/R and then inserted into the pRFHUE-eGFP vector (Crespo-Sempere et al. 2011). The resulting recombinant vector was inserted into the WT strain via *A. tumefaciens*-mediated transformation as described above. The generated overexpression transformants were identified by PCR and sequencing.

Sequence analysis

The full *GET2* gene sequences from different organisms and the encoded aa sequences were obtained from the National Center for Biotechnology Information database (<https://www.ncbi.nlm.nih.gov/>). All aa sequences were aligned using the CLUSTALW program (<https://www.genome.jp/tools-bin/clustalw>). Transmembrane helices in FgGET2 were predicted using TMHMM (<http://services.healthtech.dtu.dk/servise.php?TMHMM-2.0>).

Yeast complementation assay

Yeast strain BY4741 and its $\Delta ScGET2$ mutant were ordered from HORIZON (Dublin, Ireland). The full *ScGET2* and *FgGET2* coding sequences were amplified

by PCR using BY4741 and *F. graminearum* and primer pairs pYES2-ScGET2-F/R and pYES2-FgGET2-F/R, respectively. The amplified products were ligated into the pYES2 vector (Thermo Fisher Scientific, Waltham, MA, USA). The resulting recombinant vectors (pYES2-ScGET2 and pYES2-FgGET2) were inserted into $\Delta ScGET2$. The BY4741 and $\Delta ScGET2$ strains transformed with the empty pYES2 vector were used as controls. Yeast transformants were selected on a synthetic medium lacking uracil (Clontech, Mountain View, CA, USA). For the complementation assay, tenfold serial dilutions of yeast transformants were added to solid YEPD medium supplemented with different chemicals, including hydroxyurea, tunicamycin, hygromycin, and $CuSO_4$ (concentrations indicated in figure legends). For the heat sensitivity assay, yeast strains were grown at 39°C. All experiments were repeated independently three times.

Fungal pathogenicity in wheat spikes and DON production

To evaluate FHB symptoms in wheat, susceptible *Triticum aestivum* cultivar ‘SM482’ plants were inoculated. Plants were grown in a climate-controlled greenhouse under a 12-h (25°C) day:12-h (20°C) night cycle. At the mid-anthesis stage, two fully developed florets of a single central spikelet were inoculated with 1×10^3 conidia using a micropipette. The inoculated heads were capped with a plastic bag for 48 h to maintain moisture and incubated at 25°C. The fungal biomass in the inoculated spikelets at 2 dpi was measured by performing a qRT-PCR analysis. Visual FHB disease symptoms on 10–20 inoculated spikes per treatment were assessed at 12 dpi. To investigate pathogenicity changes in detail, fungal penetration behavior on cellophane membranes was examined as previously described (Lopez-Berges et al. 2010).

To determine the effect of *FgGET2* on the accumulation of DON in wheat spikes, each floret of a whole spike was inoculated with 1×10^3 conidia of WT or mutant strains. At least five heads per strain were analyzed. The infected spikes were harvested at 8 dpi and ground to a fine powder in liquid nitrogen. DON production was measured using a competitive ELISA-based DON detection kit (Mlbio, Shanghai, China) and a Multiskan Spectrum instrument (Thermo Fisher) as described by Qi et al. (2019). A two-stage protocol (Miller et al. 1986; Qi et al. 2012) was used to determine whether *FgGET2* is required for the production of DON in liquid medium.

Microscopic examination

Hypal morphology was examined using fresh WT and $\Delta FgGET2$ mycelia collected from 2-day-old colonies on PDA medium. Mycelia were fixed in 2.5% (v/v)

glutaraldehyde, dehydrated using a graded ethanol series, and embedded in Epon812 resin (Sigma-Aldrich, St. Louis, MO, USA). Ultrathin sections were prepared using an EM UC7 ultramicrotome (Leica, Wetzlar, Germany), after which specimens were stained with uranyl acetate and lead citrate. Hyphal morphology was observed using an HT7700 120 kV transmission electron microscope (Hitachi, Tokyo, Japan).

To examine vacuole morphology, the conidia of each strain were cultured in potato dextrose broth medium (Aobox) for 24 h. Hyphae were stained with 10 μ M (final concentration) CMAC for 30 min at 37°C as previously described (Shoji et al. 2006). The *F. graminearum* strain expressing the FgGET2-eGFP fusion was utilized for localizing FgGET2 within cells. Conidia were collected from CMC medium and germinated in YEPD medium for 6 and 24 h, after which fluorescence was examined. ER-Tracker Red was used to label the ER of hyphae as described by Yun et al. (2020). Fluorescence was detected under UV light using an Olympus-BX63 fluorescence microscope with a cooled CCD camera (DP80; Olympus, Tokyo, Japan).

Statistical analysis

All experimental data were collected from three independent samples. The significance of the differences between treatments was determined according to Student's *t*-test implemented using the Data Procension System program (version 12.01; Zhejiang University, Hangzhou, China).

Abbreviations

aa	Amino acid
Blast	Basic local alignment search tool
bp	Base pair
CD	Cytosolic domain
CMAC	7-Amino-4-chloromethylcoumarin
CR	Congo red
DON	Deoxynivalenol
dpi	Days post-inoculation
DTT	Dithiothreitol
ER	Endoplasmic reticulum
FHB	Fusarium head blight
GET	Guided entry of tail-anchored proteins
GFP	Green fluorescent protein
HPH	Hygromycin phosphotransferase
KO	Knock-out
MMS	Methyl methanesulfonate
NEO	Neomycin
SDS	Sodium dodecyl sulfate
TA	Tail-anchored
TMD	Transmembrane domain
WT	Wild type

Supplementary Information

The online version contains supplementary material available at <https://doi.org/10.1186/s42483-025-00327-3>.

Additional file 1: Table S1. Primers used in this study.

Acknowledgements

The authors thank Weihua Tang from the Institute of Plant Physiology and Ecology, Chinese Academy of Sciences for offering the JM45 vector. We thank Liwen Bianji (Edanz) (www.liwenbianji.cn) for editing the English text of a draft of this manuscript.

Author contributions

YW and PQ designed the experiments. CL, LL, JZ, ZZ, and LK performed the experiments. CL and PQ wrote the manuscript and analyzed the data. MZ, SP, JT, and LC prepared the figures. QC, YJ, GC, QJ, YZ (Yazhou Zhang), XQ, YZ (Youliang Zheng), and KK provided key reagents and advice. All authors reviewed the results and approved the final version of the manuscript.

Funding

This research was supported by the National Natural Science Foundation of China (grant numbers 32072054, 32102298, and 31901961).

Data availability

Not applicable.

Declarations

Ethics approval and consent to participate

Not applicable.

Consent for publication

Not applicable.

Competing interests

The authors declare no competing interests.

Author details

¹State Key Laboratory of Crop Gene Exploration and Utilization in Southwest China, Sichuan Agricultural University, Chengdu 611130, China. ²Triticeae Research Institute, Sichuan Agricultural University, Chengdu 611130, China. ³Institute of Phytopathology, Research Centre for Biosystems, Land Use and Nutrition, Justus Liebig University Giessen, Heinrich-Buff-Ring 26, 35392 Giessen, Germany. ⁴Institut de Biologie Moléculaire Des Plantes, CNRS, Université de Strasbourg, 12 Rue du Général Zimmer, 67084 Strasbourg, France.

Received: 2 August 2024 Accepted: 18 February 2025

Published online: 24 April 2025

References

- Asseck LY, Mehlhorn G, Rivera Monroy J, Ricardi M, Breuninger H, Wallm-eroth N, et al. Endoplasmic reticulum membrane receptors of the GET pathway are conserved throughout eukaryotes. *Proc Natl Acad Sci USA*. 2021;118(1):e2017636118. <https://doi.org/10.1073/pnas.2017636118>.
- Auld KL, Brown CR, Casolari JM, Komili S, Silver PA. Genomic association of the proteasome demonstrates overlapping gene regulatory activity with transcription factor substrates. *Mol Cell*. 2006;21(6):861–71. <https://doi.org/10.1016/j.molcel.2006.02.020>.
- Borgese N. Searching for remote homologs of CAML among eukaryotes. *Traf fic*. 2020;21(10):647–58. <https://doi.org/10.1111/tra.12758>.
- Borgese N, Fasana E. Targeting pathways of C-tail-anchored proteins. *Biochim Biophys Acta*. 2011;1808(3):937–46. <https://doi.org/10.1016/j.bbamem.2010.07.010>.
- Bryda EC, Johnson NT, Ohlemiller KK, Besch-Williford CL, Moore E, Bram RJ. Conditional deletion of calcium-modulating cyclophilin ligand causes

- deafness in mice. *Mamm Genome*. 2012;23(3–4):270–6. <https://doi.org/10.1007/s00335-011-9381-z>.
- Cappellini RA, Peterson JL. Macroconidium formation in submerged cultures by a nonsporulating strain of *Gibberella Zeae*. *Mycologia*. 1965;57(6):962–6. <https://doi.org/10.1080/00275514.1965.12018285>.
- Carvalho HJF, Del Bondio A, Maltecca F, Colombo SF, Borgese N. The WRB subunit of the Get3 receptor is required for the correct integration of its partner CAML into the ER. *Sci Rep*. 2019;9(1):11887. <https://doi.org/10.1038/s41598-019-48363-2>.
- Chang YW, Chuang YC, Ho YC, Cheng MY, Sun YJ, Hsiao CD, et al. Crystal structure of Get4-Get5 complex and its interactions with Sgt2, Get3, and Ydj1. *J Biol Chem*. 2010;285(13):9962–70. <https://doi.org/10.1074/jbc.M109.087098>.
- Chen Y, Kistler HC, Ma Z. Annual review of phytopathology *Fusarium graminearum* trichothecene mycotoxins: biosynthesis, regulation, and management. *Annu Rev Phytopathol*. 2019;57:15–39. <https://doi.org/10.1146/annurev-phyto-082718-100318>.
- Chio US, Cho H, Shan SO. Mechanisms of tail-anchored membrane protein targeting and insertion. *Annu Rev Cell Dev Biol*. 2017;33:417–38. <https://doi.org/10.1146/annurev-cellbio-100616-060839>.
- Chong X, Wang C, Wang Y, Wang Y, Zhang L, Liang Y, et al. The dynamin-like GTPase FgSey1 plays a critical role in fungal development and virulence in *Fusarium graminearum*. *Appl Environ Microbiol*. 2020;19;86(11):e02720-e2819. <https://doi.org/10.1128/AEM.02720-19>.
- Crespo-Sempere A, López-Pérez M, Martínez-Culebras PV, González-Candelas L. Development of a green fluorescent tagged strain of *Aspergillus carbonarius* to monitor fungal colonization in grapes. *Int J Food Microbiol*. 2011;148(2):135–40. <https://doi.org/10.1016/j.ijfoodmicro.2011.05.021>.
- Dean R, Van Kan JAL, Pretorius ZA, Hammond-Kosack KE, Di Pietro A, Spanu PD, et al. The Top 10 fungal pathogens in molecular plant pathology. *Mol Plant Pathol*. 2012;13(4):414–30. <https://doi.org/10.1111/j.1364-3703.2011.00783.x>.
- Dimmer KS, Fritz S, Fuchs F, Messerschmitt M, Weinbach N, Neupert W, et al. Genetic basis of mitochondrial function and morphology in *Saccharomyces cerevisiae*. *Mol Biol Cell*. 2002;13(3):847–53. <https://doi.org/10.1091/mbc.01-12-0588>.
- Duan Y, Lu F, Zhou Z, Zhao H, Zhang J, Mao Y, et al. Quinone outside inhibitors affect DON biosynthesis, mitochondrial structure and toxosome formation in *Fusarium graminearum*. *J Hazard Mater*. 2020;398: 122908. <https://doi.org/10.1016/j.jhazmat.2020.122908>.
- Enyenihi AH, Saunders WS. Large-scale functional genomic analysis of sporulation and meiosis in *Saccharomyces cerevisiae*. *Genetics*. 2003;163(1):47–54. <https://doi.org/10.1093/genetics/163.1.47>.
- Helsen J, Voordeckers K, Vanderwaeren L, Santermans T, Tsontaki M, Verstrepen KJ, et al. Gene loss predictably drives evolutionary adaptation. *Mol Biol Evol*. 2020;37(10):2989–3002. <https://doi.org/10.1093/molbev/msaa172>.
- Heo P, Culver JA, Miao J, Pincet F, Mariappan M. The Get1/2 insertase forms a channel to mediate the insertion of tail-anchored proteins into the ER. *Cell Rep*. 2023;42(1):111921. <https://doi.org/10.1016/j.celrep.2022.111921>.
- Hou Z, Xue C, Peng Y, Katan T, Corby Kistler H, Xu JR. A mitogen-activated protein kinase gene (MGV1) in *Fusarium graminearum* is required for female fertility, heterokaryon formation, and plant infection. *Mol Plant Microbe Interact*. 2002;15(11):1119–27. <https://doi.org/10.1094/MPMI.2002.15.11.1119>.
- Hughes TR, Marton MJ, Jones AR, Roberts CJ, Stoughton R, Armour CD, et al. Functional discovery via a compendium of expression profiles. *Cell*. 2000;102(1):109–26. [https://doi.org/10.1016/s0092-8674\(00\)00015-5](https://doi.org/10.1016/s0092-8674(00)00015-5).
- Jiang C, Zhang C, Wu C, Sun P, Hou R, Liu H, et al. TR16 and TR10 play different roles in the regulation of deoxynivalenol (DON) production by cAMP signalling in *Fusarium graminearum*. *Environ Microbiol*. 2016;18(11):3689–701. <https://doi.org/10.1111/1462-2920.13279>.
- Jiang J, Liu X, Yin Y, Ma Z. Involvement of a velvet protein FgVeA in the regulation of asexual development, lipid and secondary metabolisms and virulence in *Fusarium graminearum*. *PLoS ONE*. 2011;6(11):e28291. <https://doi.org/10.1371/journal.pone.0028291>.
- Jonikas MC, Collins SR, Denic V, Oh E, Quan EM, Schmid V, et al. Comprehensive characterization of genes required for protein folding in the endoplasmic reticulum. *Science*. 2009;323(5922):1693–7. <https://doi.org/10.1126/science.1167983>.
- Kiktev DA, Patterson JC, Müller S, Bariar B, Pan T, Chernoff YO. Regulation of chaperone on a yeast prion by cochaperone Sgt2. *Mol Cell Biol*. 2012;32(24):4960–70. <https://doi.org/10.1128/mcb.00875-12>.
- Kumar T, Maitra S, Rahman A, Bhattacharjee S. A conserved guided entry of tail-anchored pathway is involved in the trafficking of a subset of membrane proteins in *Plasmodium falciparum*. *PLoS Pathog*. 2021;17(11):e1009595. <https://doi.org/10.1371/journal.ppat.1009595>.
- Li G, Zhou J, Jia H, Gao Z, Fan M, Luo Y, et al. Mutation of a histidine-rich calcium-binding-protein gene in wheat confers resistance to *Fusarium head blight*. *Nat Genet*. 2019;51(7):1106–12. <https://doi.org/10.1038/s41588-019-0426-7>.
- Livak KJ, Schmittgen TD. Analysis of relative gene expression data using real-time quantitative PCR and the 2^{(-Delta Delta C(T))} Method. *Methods*. 2001;25(4):402–8. <https://doi.org/10.1006/meth.2001.1262>.
- López-Berges MS, Rispaill N, Prados-Rosales RC, di Pietro A. A nitrogen response pathway regulates virulence functions in *Fusarium oxysporum* via the protein kinase TOR and the bZIP protein MeaB. *Plant Cell*. 2010;22(7):2459–75. <https://doi.org/10.1105/tpc.110.075937>.
- Maier FJ, Malz S, Lösch AP, Lacour T, Schäfer W. Development of a highly efficient gene targeting system for *Fusarium graminearum* using the disruption of a polyketide synthase gene as a visible marker. *FEMS Yeast Res*. 2005;5(6–7):653–62. <https://doi.org/10.1016/j.femsyr.2004.12.008>.
- Mateja A, Keenan RJ. A structural perspective on tail-anchored protein biogenesis by the GET pathway. *Curr Opin Struct Biol*. 2018;51:195–202. <https://doi.org/10.1016/j.sbi.2018.07.009>.
- McDowell MA, Heimes M, Fiorentino F, Mehmood S, Farkas Á, Coy-Vergara J, et al. Structural basis of tail-anchored membrane protein biogenesis by the GET insertase complex. *Mol Cell*. 2020;80(1):72–86. <https://doi.org/10.1016/j.molcel.2020.08.012>.
- Miller JD, Blackwell BA. Biosynthesis of 3-acetyldeoxynivalenol and other metabolites by *Fusarium culmorum* HLX 1503 in a stirred jar fermentor. *Can J Bot*. 1986;64(1):1–5. <https://doi.org/10.1139/b86-001>.
- Okreglak V, Walter P. The conserved AAA-ATPase Msp1 confers organelle specificity to tail-anchored proteins. *Proc Natl Acad Sci U S A*. 2014;111(22):8019–24. <https://doi.org/10.1073/pnas.1405755111>.
- Onishi M, Nagumo S, Iwashita S, Okamoto K. The ER membrane insertase Get1/2 is required for efficient mitophagy in yeast. *Biochem Biophys Res Commun*. 2018;503(1):14–20. <https://doi.org/10.1016/j.bbrc.2018.04.114>.
- Osborne LE, Stein JM. Epidemiology of *Fusarium head blight* on small-grain cereals. *Int J Food Microbiol*. 2007;119(1–2):103–8. <https://doi.org/10.1016/j.ijfoodmicro.2007.07.032>.
- Qi PF, Johnston A, Balcerzak M, Rocheleau H, Harris LJ, Long XY, et al. Effect of salicylic acid on *Fusarium graminearum*, the major causal agent of *Fusarium head blight* in wheat. *Fungal Biol*. 2012;116(3):413–26. <https://doi.org/10.1016/j.funbio.2012.01.001>.
- Qi PF, Zhang YZ, Liu CH, Chen Q, Guo ZR, Wang Y, et al. Functional analysis of FgNahG clarifies the contribution of salicylic acid to wheat (*Triticum aestivum*) resistance against *Fusarium head blight*. *Toxins (Basel)*. 2019;11(2):59. <https://doi.org/10.3390/toxins11020059>.
- Riquelme M, Aguirre J, Bartnicki-García S, Braus GH, Feldbrügge M, Fleig U, et al. Fungal morphogenesis, from the polarized growth of hyphae to complex reproduction and infection structures. *Microbiol Mol Biol Rev*. 2018;82(2):e00068–17. <https://doi.org/10.1128/MMBR.00068-17>.
- Ruotolo R, Marchini G, Ottonello S. Membrane transporters and protein traffic networks differentially affecting metal tolerance: a genomic phenotyping study in yeast. *Genome Biol*. 2008;9(4):R67. <https://doi.org/10.1186/gb-2008-9-4-r67>.
- Schuldiner M, Metz J, Schmid V, Denic V, Rakwalska M, Schmitt HD, et al. The GET complex mediates insertion of tail-anchored proteins into the ER membrane. *Cell*. 2008;134(4):634–45. <https://doi.org/10.1016/j.cell.2008.06.025>.
- Shoji JY, Arioka M, Kitamoto K. Vacuolar membrane dynamics in the filamentous fungus *Aspergillus oryzae*. *Eukaryot Cell*. 2006;5(2):411–21. <https://doi.org/10.1128/EC.5.2.411-421.2006>.
- Smith SJ, Crowley JH, Parks LW. Transcriptional regulation by ergosterol in the yeast *Saccharomyces cerevisiae*. *Mol Cell Biol*. 1996;16(10):5427–32. <https://doi.org/10.1128/MCB.16.10.5427>.
- Stefer S, Reitz S, Wang F, Wild K, Pang YY, Schwarz D, et al. Structural basis for tail-anchored membrane protein biogenesis by the Get3-receptor complex. *Science*. 2011;333(6043):758–62. <https://doi.org/10.1126/science.1207125>.

- Suloway CJM, Rome ME, Clemons WM. Tail-anchor targeting by a Get3 tetramer: the structure of an archaeal homologue. *EMBO J*. 2012;31(3):707–19. <https://doi.org/10.1038/emboj.2011.433>.
- Su Z, Bernardo A, Tian B, Chen H, Wang S, Ma H, et al. A deletion mutation in *TaHRC* confers *Fhb1* resistance to Fusarium head blight in wheat. *Nat Genet*. 2019;51(7):1099–105. <https://doi.org/10.1038/s41588-019-0425-8>.
- Tran DD, Russell HR, Sutor SL, van Deursen J, Bram RJ. CAML is required for efficient EGF receptor recycling. *Dev Cell*. 2003;5(2):245–56. [https://doi.org/10.1016/s1534-5807\(03\)00207-7](https://doi.org/10.1016/s1534-5807(03)00207-7).
- Vidal A, Claeys L, Mengelers M, Vanhoorne V, Vervaeke C, Huybrechts B, et al. Humans significantly metabolize and excrete the mycotoxin deoxynivalenol and its modified form deoxynivalenol-3-glucoside within 24 hours. *Sci Rep*. 2018;8(1):5255. <https://doi.org/10.1038/s41598-018-23526-9>.
- Vilardi F, Lorenz H, Dobberstein B. WRB is the receptor for TRC40/Asna1-mediated insertion of tail-anchored proteins into the ER membrane. *J Cell Sci*. 2011;124(8):1301–7. <https://doi.org/10.1242/jcs.084277>.
- Wang F, Whynot A, Tung M, Denic V. The mechanism of tail-anchored protein insertion into the ER Membrane. *Mol Cell*. 2011;43(5):738–50. <https://doi.org/10.1016/j.molcel.2011.07.020>.
- Winzeler EA, Shoemaker DD, Astromoff A, Liang H, Anderson K, Andre B, et al. Functional characterization of the *S. cerevisiae* genome by gene deletion and parallel analysis. *Science*. 1999;285(5429):901–6. <https://doi.org/10.1126/science.285.5429.901>.
- Xu X, Nicholson P. Community ecology of fungal pathogens causing wheat head blight. *Annu Rev Phytopathol*. 2009;47:83–103. <https://doi.org/10.1146/annurev-phyto-080508-081737>.
- Yu F, Gu Q, Yun Y, Yin Y, Xu JR, Shim WB, et al. The TOR signaling pathway regulates vegetative development and virulence in *Fusarium graminearum*. *New Phytol*. 2014;203(1):219–32. <https://doi.org/10.1111/nph.12776>.
- Yamamoto Y, Sakisaka T. Molecular machinery for insertion of tail-anchored membrane proteins into the endoplasmic reticulum membrane in mammalian cells. *Mol Cell*. 2012;48(3):387–97. <https://doi.org/10.1016/j.molcel.2012.08.028>.
- Zalisko BE, Chan C, Denic V, Rock RS, Keenan RJ. Tail-anchored protein insertion by a single Get1/2 heterodimer. *Cell Rep*. 2017;20(10):2287–93. <https://doi.org/10.1016/j.celrep.2017.08.035>.
- Zewail A, Xie MW, Xing Y, Lin L, Zhang PF, Zou W, et al. Novel functions of the phosphatidylinositol metabolic pathway discovered by a chemical genomics screen with wortmannin. *Proc Natl Acad Sci U S A*. 2003;100(6):3345–50. <https://doi.org/10.1073/pnas.0530118100>.